Journal of Rajasthan Academy of Physical Sciences
ISSN : 0972-6306; URL : http://raops.org.in
Vol. 12, No. 2, June 2013, pp 181-198

HEAT TRANSFER AND ENTROPY GENERATION ON MHD SQUEEZING FLOW BETWEEN TWO PARALLEL ROTATING PLATES USING BRINKMAN MODEL

S.C. RAJVANSHI
Department of Applied Sciences,
Gurukul Vidyapeeth Institute of Engineering & Technology,
Sector # 7, Banur-140601, Distt Patiala, Punjab, India
E-mail : satishrajvanshi@yahoo.com

B.S. SAINI
Department of Applied Sciences,
Gurukul Vidyapeeth Institute of Engineering & Technology,
Sector # 7, Banur-140601, Distt Patiala, Punjab, India
E-mail : bssmaths@rediffmail.com

SARGAM WASU
Department of Applied Sciences,
R.B. Institute of Engineering & Biotechnology,
Sahauran, Kharar-140104, Distt Mohali, Punjab, India

Recieved : March 15, 2013

Abstract : The squeezing flow of viscous incompressible fluid in a highly permeable medium between two parallel, permeable rotating plates has been investigated. The plates at time t^* are separated by a distance $H(1-\alpha t^*)^{1/2}$. These are rotating with angular velocities proportional to $\Omega_i(1-\alpha t^*)^{-1}$, $i=1,2$ for lower and upper plate respectively. The effect of permeability and magnetic parameter on the temperature, heat transfer and entropy generation is investigated and discussed.

Keywords and Phrases. Squeezing flow, Permeable plates, Porous medium, Heat transfer, Entropy, MHD.

2010 Mathematics Subject Classification : 76D99; 76S99; 76W05

1. Introduction

The study of fluid flow problems based on flow between rotating porous boundaries have vast implications in the development of lubrication theory and hydraulics. The unsteady squeezing flow of a viscous incompressible fluid between two parallel plates

moving normal to their own planes occurs in many hydro-dynamical machines, particularly in turbo-machinery.

These squeezing flows are useful in polymer processing, compression and injection moulding. Earlier studies of squeezing flows involved the solution of Reynolds equation. The study involving full Navier-Stokes equations is more useful in the analysis of porous thrust bearing and squeeze films involving high velocities.

The system of rotating plates as an idealized model of a turbo machinery unit especially, in the case where one plate is set in rotation while the other is stationary, was considered by Lygren and Andersson [11]. Kuhn and Yates [10] examined the pressure distribution of a thin liquid film between axially oscillating parallel circular plates by taking inertia terms into account. They also utilized the method of least squares to fit a third order polynomial to experimental values of maximum pressure. The pressure distribution in a plane fluid film subject to normal sinusoidal excitation has been studied by Hunt [9]. He has shown that the maximum and minimum pressures in the fluid depend on the amplitude of oscillation. A correlation between theoretical and experimental work was also brought out by him. Terrill [19] gave an analytic solution of the Navier Stokes equation for flow between two parallel plates, one of which was subjected to normal sinusoidal oscillation. He showed that the solution depends upon the non-dimensional amplitude of the oscillation of the disk and the Reynolds number related to the maximum velocity of the oscillating disk.

Rajvanshi [14] considered the flow between two parallel plates, when both perform normal sinusoidal oscillations. He observed that the solution depends on the amplitude of the oscillation of the plates and the Reynolds number related to the maximum velocity of the normal oscillations. Saini [18] studied the flow between two parallel plates, one of which was subjected to normal sinusoidal oscillations and the other highly permeable. He presented the detailed solution of Navier-Stokes equations for the following two cases:

(i) Reynolds number Re related to maximum normal velocity of the oscillating plate is so small that inertia terms are neglected, and

(ii) for small Re.

Rajvanshi [15] also studied the effect of slip velocity in the axial current induced pinch effect on the squeeze-film behavior on annular plates with the assumption of hydromagnetic lubrication in the Navier-Stokes equations. The effect of slip velocity and axial current induced pinch on load capacity and film thickness-time was explicitly recorded.

Aristov and Gitman [1] studied the motion of liquids through hydraulic pumps and motion of underground water. They described the motion of fluid in a hydraulic pump as the motion of two impermeable plates moving towards or apart from each other. Bhatt and Hamza [2] have analyzed similarity solutions for the squeeze film between two rotating naturally permeable plates. The plate permeabilities were taken as $k_i(1-\alpha t^*)$ at any time t^*, $i=1,2$ for the lower and upper plates respectively. They studied the effect of rotation and permeabilities on velocity profiles. A similarity solution for the Navier-Stokes equations has been presented for the unsteady flow between two plates approaching or receding from each other symmetrically by Gupta and Gupta [6]. Rashidi *et al* [16] investigated the flow due to the normal motion of the two parallel plates placed at a distance $z=\pm l(1-\alpha t)^{1/2}$ apart. The Navier-Stokes equations are reduced to a fourth order nonlinear differential equation by using similarity solutions. The resulting equation has been solved by homotopy analysis method. Rukmani and Usha [17] have studied arbitrary squeezing flow between two plates of varying gap-width. The solution is obtained as a power series in a non-dimensional squeeze number. The gap-width is obtained for the cases when the top plate moves with constant velocity, constant force or constant power.

Mohais [12] examined the MHD squeeze flow between two permeable parallel rotating plates in presence of a magnetic field. She has assumed that a plate separation of $H(1-\alpha t^*)^{1/2}$ exists at time t^*, where H and α^{-1} denote characteristic length and time respectively. She has studied temperature and heat transfer profiles, when

(i) each plate is set at a constant temperature, and

(ii) upper plate is maintained at a constant uniform temperature and the lower plate is subjected to heat flux.

Usha and Vasudevan [20] have studied the flow between two rotating parallel plates in the presence of a magnetic field using similarity solution. They observed that by increasing the magnetic force, an increase in the load can be achieved. Recently, Hayat *et al* [8] have studied the MHD squeezing flow of a second grade fluid between two parallel plates.

In the present times, there is a dire need to conserve and utilize energy in all thermodynamic systems. The heat transfer processes involve thermodynamic irreversibility which is related to entropy generation. The uses of microelectronic devices involve heat transfer through electrically conducting fluids under the effect of magnetic

field. The study of entropy generation may be used to enhance the efficiency of these devices and develop new designs. The influence of MHD over rotating plates has applications in the manufacture of computer disk drives and many other related electronic devices. The entropy generation has been studied during fluid flow between two parallel plates with moving bottom by Erbay *et al* [5]. Chauhan and Kumar [4] have also conducted studies of heat transfer effects on fluid flow through porous medium by incorporating entropy analysis. The effect of slip on entropy generation in a single rotating disk in MHD flow has been investigated by Ozkol *et al* [13].

In the present investigation, the MHD squeezing flow of a viscous incompressible fluid in a highly permeable porous medium contained between two permeable rotating plates is being studied using the Brinkman model. The problem has applications to special porous media such as mushy zones and ferromagnetic fluids where the magnetic drag plays a significant role. The plates are rotating with angular velocities proportional to $\Omega_i(1-\alpha t^*)^{-1}, i=1,2$ for the lower and upper plate respectively. The upper and the lower plates are maintained at different temperatures. A perturbation solution has been obtained in powers of squeeze flow Reynolds number. The effect of permeability and magnetic parameter on the temperature, heat transfer profiles and entropy generation is investigated.

2. Formulation of the problem

We consider a thin film of a highly permeable medium saturated with Newtonian fluid squeezed between two parallel plates with different permeability. The plates placed at a distance $h(t^*)$ at any time t^*, in an orthogonally applied magnetic field $B(t^*)$ are allowed to rotate in their own planes about the z^*-axis with different angular velocities. The plates are made of non-conducting material, so that there are no eddy currents in the system. The upper plate is set in motion along the z^*-axis with velocity $\frac{dz^*}{dt^*}$ towards the lower plate which remains at a fixed position $z^*=0$.

The governing equations for flow through porous medium as suggested by Brinkman [3] are

$$\frac{\partial u^*}{\partial r^*}+\frac{u^*}{r^*}+\frac{\partial w^*}{\partial z^*}=0 \tag{1}$$

$$\frac{\partial u^*}{\partial t^*}+u^*\frac{\partial u^*}{\partial r^*}+w^*\frac{\partial u^*}{\partial z^*}-\frac{v^{*2}}{r^*}=-\frac{1}{\rho}\frac{\partial p}{\partial r^*}+\bar{\nu}\left(\frac{\partial^2 u^*}{\partial r^{*2}}+\frac{1}{r^*}\frac{\partial u^*}{\partial r^*}-\frac{u^*}{r^{*2}}+\frac{\partial^2 u^*}{\partial z^{*2}}\right)-\frac{\nu u^*}{k}-\frac{\sigma B u^*}{\rho} \tag{2}$$

$$\frac{\partial v^*}{\partial t^*}+\frac{u^*v^*}{r^*}+u^*\frac{\partial v^*}{\partial r^*}+w^*\frac{\partial v^*}{\partial z^*}=\bar{\upsilon}\left(\frac{1}{r^*}\frac{\partial v^*}{\partial r^*}-\frac{v^*}{r^{*2}}+\frac{\partial^2 v^*}{\partial r^{*2}}+\frac{\partial^2 v^*}{\partial z^{*2}}\right)-\frac{\upsilon\, v^*}{k}-\frac{\sigma B^2 v^*}{\rho} \tag{3}$$

$$\frac{\partial w^*}{\partial t^*}+u^*\frac{\partial w^*}{\partial r^*}+w^*\frac{\partial w^*}{\partial z^*}=-\frac{1}{\rho}\frac{\partial p}{\partial z^*}+\bar{\upsilon}\left(\frac{\partial^2 w^*}{\partial r^{*2}}+\frac{1}{r^*}\frac{\partial w^*}{\partial r^*}+\frac{\partial^2 w^*}{\partial z^{*2}}\right)-\frac{\upsilon}{k}w^* \tag{4}$$

$$\rho C_p\left(\frac{\partial T^*}{\partial t^*}+u^*\frac{\partial T^*}{\partial r^*}+w^*\frac{\partial T^*}{\partial z^*}\right)=\bar{\kappa}\left[\frac{1}{r^*}\frac{\partial}{\partial r^*}\left(r^*\frac{\partial T^*}{\partial r^*}\right)+\frac{\partial^2 T^*}{\partial z^{*2}}\right] \tag{5}$$

where u^*, v^*, w^* are the velocity components in the direction of r^*, θ^* and z^* respectively, p the pressure, υ the kinematic viscosity, $\bar{\upsilon}$ the effective kinematic viscosity in porous medium, σ the electrical conductivity, C_p the specific heat at constant pressure, k the permeability of the porous medium, $\bar{\kappa}$ the effective thermal conductivity in porous medium, ρ the fluid density, and B the magnetic field. Owing to symmetrical considerations $\frac{\partial}{\partial \theta^*}(\,) = 0$

With a view to make the physical quantities dimensionless, we introduce the characteristic length, time and angular velocity H, α^{-1} and Ω respectively. The lower and the upper plate are assumed to rotate with angular velocities $\Omega_1(1-\alpha t^*)^{-1}$ and $\Omega_2(1-\alpha t^*)^{-1}$ respectively. The permeabilities of lower plate, upper plate and porous medium are taken in the form $k_1(1-\alpha t^*)$, $k_2(1-\alpha t^*)$ and $k_0(1-\alpha t^*)$ respectively.

The boundary conditions on the plates are assumed in the form

$$\frac{\partial u^*}{\partial z^*}=\frac{\sigma_1 u^*}{\sqrt{k_1^*}},\quad \frac{\partial v^*}{\partial z^*}=\frac{\sigma_1}{\sqrt{k_1^*}}\left(v^*-\frac{\Omega_1 r^*}{1-\alpha t^*}\right),\quad w^*=0,\ \text{on}\ z^*=0$$

$$\frac{\partial u^*}{\partial z^*}=\frac{-\sigma_2 u^*}{\sqrt{k_2^*}},\quad \frac{\partial v^*}{\partial z^*}=\frac{-\sigma_2}{\sqrt{k_2^*}}\left(v^*-\frac{\Omega_2 r^*}{1-\alpha t^*}\right),\quad w^*=\frac{dh}{dt^*},\ \text{on}\ z^*=h(t^*) \tag{6}$$

where σ_1 and σ_2 represents slip parameters for lower and upper disk respectively.

Following Wang [21] we introduce the following non-dimensional quantities

$$u^*(y)=\frac{\alpha r^* f'(y)}{2(1-\alpha t^*)},\quad v^*(y)=\frac{r^*\Omega g(y)}{(1-\alpha t^*)},\quad w^*(y)=\frac{-\alpha H f(y)}{\sqrt{1-\alpha t^*}} \tag{7}$$

and

$$B = \frac{B_0}{\sqrt{1-\alpha t^*}} \tag{8}$$

The temperature T^* is given by

$$T^* = \frac{T_0 a(y)}{1-\alpha t^*} + T_0 \tag{9}$$

where

$$y = \frac{z^*}{H\sqrt{1-\alpha t^*}} \tag{10}$$

The following non-dimensional quantities are also introduced $\phi_1 = \frac{\bar{\upsilon}}{\upsilon}$, $\phi_2 = \frac{\bar{\kappa}}{\kappa}$,

where κ is the thermal conductivity. With a view to maintain uniformity, we replace $r^* \to r$, $z^* \to z$ and $t^* \to t$.

Using equations (7) to (10), the governing equations (2), (3), (4) and (5) take the form

$$\frac{1}{\rho}\frac{\partial p}{\partial r} = \frac{r\alpha^2}{4(1-\alpha t)^2}\left[\frac{f'''}{Re^S} - y f'' - 2f' + 2ff' - (f')^2 + N^2 g^2 - \frac{\beta f'}{Re^S}\right] \tag{11}$$

$$\frac{g''}{Re^S} - \frac{\beta g}{Re^S} - y g' - 2g - 2f'g + 2f g' = 0 \tag{12}$$

$$\frac{1}{\rho}\frac{\partial p}{\partial y} = \frac{-\alpha^2 H}{2(1-\alpha t)}\left[\frac{f''}{Re^S} - y f' - f' + 2ff' - 2\lambda_4 f\right] \tag{13}$$

$$\frac{\phi_2 a''}{\phi_1 Pr\, Re^S} + 2 f a' - a' y - 2a = 0 \tag{14}$$

where $M^2 = (H B_0)^2 \sigma \mu^{-1}$, Re^S(Squeeze Reynolds Number) $= \frac{\rho \alpha H^2}{2\bar{\mu}}$, $N = \frac{2\Omega}{\alpha}$, $\lambda_3 = \frac{H}{\sqrt{k_0}}$, $\lambda_4 = \frac{\upsilon}{\alpha k_0}$, $\beta = \frac{1}{\phi_1}(\lambda_3^2 + M^2)$.

Equation (1) is satisfied identically by the velocity components.

N may also be interpreted as follows

$$N = \frac{2\Omega}{\alpha} = \frac{Re^R}{Re^S}$$

where $Re^R = \frac{\rho \Omega H^2}{\mu}$ is rotational Reynolds number. Therefore N defines the ratio of Rotational Reynolds number to Squeeze Reynolds number.

Equation (13) implies that

$$\frac{\partial^2 p}{\partial y \partial r} = 0 \tag{15}$$

Equation (11) gives

$$\frac{\partial^2 p}{\partial y \partial r} = \frac{\rho r \alpha^2}{4(1-\alpha t)^2}\left[\frac{f^{iv}}{Re^s} - 3f'' - yf''' + 2ff''' + 2N^2 gg' - \frac{\beta f''}{Re^s}\right] \tag{16}$$

Equations (15) and (16) imply

$$f^{iv} = Re^s(3f'' + yf''' - 2ff''' - 2N^2 gg') + \beta f'' \tag{17}$$

It is assumed that the plates are maintained at different temperatures given by

$T^* = T_0$ at $z^* = 0$, and

$$T^* = T_0 + \frac{T_0}{(1-\alpha t^*)} \text{ at } z^* = h(t^*) \tag{18}$$

The modified boundary conditions are

$$f''(0) = \lambda_1 f'(0), \quad g'(0) = \lambda_1\{g(0) - 1\}, \quad f(0) = 0, a(0) = 0$$

$$f''(1) = -\lambda_2 f'(1), \quad g'(1) = -\lambda_2\{g(1) - s\}, \quad f(1) = 1/2, a(1) = 1 \tag{19}$$

The slip parameters are given by

$$\lambda_i = \sigma_i H / \sqrt{k_i} \tag{20}$$

where σ_i, $i = 1, 2$ represents the slip parameter for the lower and upper plate respectively . Ratio of the rotational velocities of the plates is defined as

$$s = \Omega_2 / \Omega_1 \tag{21}$$

such that

$s = 1$, depicts that the plates are rotating with the same angular velocities in the same direction,

$s > 0$, shows that the plates are rotating in the same direction,

$s = 0$, depicts that the upper plate is stationary, and

$s < 0$, relates to the rotation of plates in opposite directions.

3. Solution of the governing equations

Governing equations are solved using regular perturbation technique. f, g and a are expanded in the following forms

$$(f, g, a) = (f_0, g_0, a_0) + \mathrm{Re}^s (f_1, g_1, a_1) + O(\mathrm{Re}^s)^2 \tag{22}$$

Equations (17), (12) and (14) give

$$f_0^{iv} = \beta f_0''' \tag{23}$$

$$f_1^{iv} = 3f_0'' + y\, f_0''' - 2f_0\, f_0''' - 2N^2 g_0 g_0' + \beta f_1'' \tag{24}$$

$$g_0'' = \beta g_0 \tag{25}$$

$$g_1'' - \beta g_1 - y\, g_0' - 2g_0 - 2f_0'\, g_0 + 2f_0 g_0' = 0 \tag{26}$$

$$a_0'' = 0 \tag{27}$$

$$a_1'' = \frac{\phi_4\, Pr}{\phi_2}(2a_0 + y\, a_0' - 2f_0 a_0') \tag{28}$$

The corresponding boundary conditions are

$$f_0(0) = 0, \quad f_1(0) = 0, \quad f_0''(0) = \lambda_1 f_0'(0), \quad f_1''(0) = \lambda_1 f_1'(0),$$

$$f_0(1) = \frac{1}{2}, \quad f_1(1) = 0, \quad f_0''(1) = -\lambda_2 f_0'(1), \quad f_1''(1) = -\lambda_2 f_1'(1), \tag{29}$$

$$g_0'(0) = \lambda_1 \{g_0(0) - 1\}, \quad g_1'(0) = \lambda_1 g_1(0),$$

$$g_0'(1) = -\lambda_2 \{g_0(1) - s\}, \quad g_1'(1) = -\lambda_2 g_1(1), \tag{30}$$

$$a_0(0) = 0, a_1(0) = 0, \quad a_0(1) = 1, a_1(1) = 0\,, \tag{31}$$

The solution of equations (23) – (28) using (29) - (31) is given by

$$f_0(y) = \gamma_{14} + y\gamma_{13} + \gamma_{12} e^{\sqrt{\beta}y} + \gamma_{11} e^{-\sqrt{\beta}y} \tag{32}$$

$$f_1(y) = \gamma_{57} + y\gamma_{56} + \gamma_{54} e^{\sqrt{\beta}y} + \gamma_{55} e^{-\sqrt{\beta}y} + \frac{y\gamma_{28} e^{\sqrt{\beta}y}}{2\beta\sqrt{\beta}} - \frac{y\gamma_{29} e^{-\sqrt{\beta}y}}{2\beta\sqrt{\beta}}$$

$$+ \frac{\gamma_{30} e^{\sqrt{\beta}y}}{2\beta\sqrt{\beta}} \left(\frac{y^2}{2} - \frac{5y}{2\sqrt{\beta}} \right) - \frac{\gamma_{31} e^{-\sqrt{\beta}y}}{2\beta\sqrt{\beta}} \left(\frac{y^2}{2} + \frac{5y}{2\sqrt{\beta}} \right) - \frac{\gamma_{32}}{12\beta^2} e^{2\sqrt{\beta}y} + \frac{\gamma_{33}}{12\beta^2} e^{-2\sqrt{\beta}y} - \frac{y^2 \gamma_{34}}{2\beta} \tag{33}$$

$$g_0(y) = \gamma_3 e^{\sqrt{\beta}y} + \gamma_4 e^{-\sqrt{\beta}y} \tag{34}$$

$$g_1(y) = \gamma_{26}e^{\sqrt{\beta}y} + \gamma_{27}e^{-\sqrt{\beta}y} + \frac{\gamma_{15}e^{\sqrt{\beta}y}}{2\sqrt{\beta}}\left(\frac{y^2}{2} - \frac{y}{2\sqrt{\beta}}\right) - \frac{\gamma_{16}e^{-\sqrt{\beta}y}}{2\sqrt{\beta}}\left(\frac{y^2}{2} + \frac{y}{2\sqrt{\beta}}\right) +$$

$$\frac{y\gamma_{17}e^{\sqrt{\beta}y}}{2\sqrt{\beta}} - \frac{y\gamma_{18}e^{-\sqrt{\beta}y}}{2\sqrt{\beta}} - \gamma_{19} \tag{35}$$

$$a_0(y) = y \tag{36}$$

$$a_1(y) = \frac{\phi_1 Pr}{\phi_2}\left[\frac{y^5}{2} - y^2\gamma_{14} - \frac{y^5\gamma_{18}}{3} - \frac{2\gamma_{12}e^{\sqrt{\beta}y} + 2\gamma_{11}e^{-\sqrt{\beta}y}}{\beta}\right] + \gamma_{59}y + \gamma_{58} \tag{37}$$

where γ_1 to γ_{59} are constants not recorded for the sake of brevity.

4. Results and discussion

Numerical work has been done by taking $N = 80, \mathrm{Re}^s = 0.02, \phi_1 = 1, \phi_2 = 1$. It is noted here that large values of λ_i corresponds to small permeabilities since $\lambda_i = \frac{\sigma_i H}{\sqrt{k_i}}$.

Temperature Profiles

Fig.1 shows the effect of the permeability of the lower plate on the temperature profiles. It is seen that temperature profiles increase with decrease in permeability of the lower plate. On the other hand, temperature profiles decrease with decrease in the permeability of the upper plate as shown in fig. 2.

Table-I: Values of *a(y)*

y	$M = 0.5$	$M = 2.5$	$M = 4$
0	0.0000	0.0000	0.0000
0.2	0.0160	0.0162	0.0164
0.4	0.0799	0.0800	0.0801
0.6	0.2361	0.2360	0.2359
0.8	0.5280	0.5278	0.5276
1.0	1.0000	1.0000	1.0000

The effect of magnetic parameter M on fluid temperature is shown in Table-I. The values have been calculated for $\mathrm{Pr} = 11.4$, $\mathrm{Re}^s = 0.02$, $\lambda_1 = \lambda_2 = 0.05, \lambda_3 = 1, s = 0.5$ and $N = 80$. The presence of magnetic field in an electrically conducting fluid introduces a force which acts against the flow and tends to slow it down. This results in increase in the temperature profile. It is further noted that the variation in M does not show significant change in the temperature. It is seen from Table-1 that fluid temperature increases with increase in the magnetic parameter in the first half and it shows reverse behavior in the second half.

Heat Transfer Profiles

Following Hamza [7], Nusselt number is defined as

$$Nu^* = -\frac{H}{T_0}\frac{\partial T}{\partial z^*} = -\frac{a'(y)}{(1-\alpha t)^{3/2}}$$

We further define

$$Nu = Nu^*(1-\alpha t)^{3/2} = -a'(y) \tag{38}$$

Fig. 3 shows heat transfer profiles on the lower plate versus λ_3 for different values of λ_1 and Prandtl number Pr. It is seen from the figure that heat transfer profiles increase with decrease in the permeability of the lower plate (as increases). With increase in Prandtl number the ratio of momentum diffusivity to thermal diffusivity increases. This leads to the increase in the heat transfer at lower plate with increase in Prandtl number . The effect of magnetic parameter versus on heat transfer profiles at the lower plate is shown in fig. 4. It is noted that heat transfer at the lower plate decreases with increase in M.

Heat transfer versus λ_3 at the upper plate is shown in fig.5 which depicts that heat transfer profiles increase with decrease in the permeability of the upper plate (as λ_2 increases). It also increases with increase in Prandtl number Pr. Fig. 6 shows the effect of magnetic parameter M on heat transfer at the upper plate. It is observed that heat transfer decreases with increase in magnetic parameter as the parameter is made to vary.

Entropy Generation

The entropy generation in the present study is written as

$$S''' = \frac{\kappa}{T_0^{*2}}\left[\left(\frac{\partial T^*}{\partial r^*}\right)^2 + \left(\frac{\partial T^*}{\partial z^*}\right)^2\right] + \frac{1}{T_0^*}\sigma B^2(u^{*2} + v^{*2}) + \frac{1}{T_0^*}\phi \tag{39}$$

where T_0^* is a reference temperature and

$$\phi = \bar{\mu}\left[2\left\langle\left(\frac{\partial u^*}{\partial r^*}\right)^2 + \left(\frac{u^*}{r^*}\right)^2 + \left(\frac{\partial w^*}{\partial z^*}\right)^2\right\rangle + \left(\frac{\partial v^*}{\partial z^*}\right)^2 + \left(\frac{\partial u^*}{\partial z^*} + \frac{\partial w^*}{\partial r^*}\right)^2 + \left(\frac{\partial v^*}{\partial r^*} - \frac{v^*}{r^*}\right)^2\right]$$

$$+ \frac{\mu}{k_0}\left[u^{*2} + v^{*2} + w^{*2}\right] \tag{40}$$

We define volumetric entropy generation in dimensionless form as

$$Ns = \frac{S'''}{S_0'''} \tag{41}$$

where

$S_0''' = \frac{\bar{\kappa}}{H^2\vartheta\eta^3}$ is reference volumetric entropy generation, $\eta = (1 - \alpha t)$, $\vartheta = \frac{T_0^*}{T_0}$ is dimensionless reference temperature, $\bar{r} = \frac{r^*}{H}$ is the dimensionless radial coordinate, $Br = \frac{\bar{\mu}\,\Omega^2 H^2}{\kappa T_0}$ is the rotational Brinkman number.

Using the equations (7) to (9) in (39) – (41) the dimensionless form of the total local entropy generation is written as the sum of local entropy generation due to heat transfer irreversibility (Ns_1), local entropy generation due to fluid friction irreversibility (Ns_2) and local entropy generation due to magnetic effect (Ns_3) in the following manner

$$Ns = Ns_1 + Ns_2 + Ns_3 \tag{42}$$

where

$$Ns_1 = \frac{\alpha'^2}{\vartheta} \tag{43}$$

$$Ns_2 = Br\left[\frac{12 f'^2\eta}{N^2} + \bar{r}^2 g'^2 + \frac{\bar{r}^2 f''^2}{N^2}\right] + \frac{\lambda_3^2 Br}{\phi_1}\left[\frac{\bar{r}^2 f'^2}{N^2} + \bar{r}^2 g^2 + \frac{4 f^2\eta}{N^2}\right] \tag{44}$$

$$Ns_3 = M^2\,\bar{r}^2\,Br\left(\frac{f'^2}{N^2} + g^2\right) \tag{45}$$

Ns_1, Ns_2 and Ns_3 can be evaluated using equations (43) - (45).

With a view to understand entropy generation mechanism of convective heat transfer an irreversibility distribution ratio ϕ is defined as

$$\Phi = \frac{(Ns_2 + Ns_2)}{Ns_1} \tag{46}$$

It is noted that heat transfer irreversibility is dominant for $0 < \Phi < 1$; fluid friction and magnetic effect dominate for $\Phi > 1$. When $\Phi = 1$, the contribution of heat transfer to entropy generation is equal to the sum of fluid friction and magnetic effects.

The effect of entropy due to heat transfer irreversibility (Ns_1) has been depicted in fig.7. It is observed that as the distance between the two plates increases the entropy generated also increases. By increasing the values of Φ_1, Φ_2 the profiles are enhanced further.

Entropy generation due to fluid friction irreversibility (Ns_2)shows a decreasing trend as the permeable upper plate moves apart. This is shown in fig. 8.

Fig.9 shows the variation of Ns_3 with y. A decreasing trend is observed for the entropy generation due to magnetic field. The total entropy also decreases as depicted in fig.10.

The variation of irreversibility distribution parameter Φ has been shown in Table-II with $\mathrm{Re}^s = 0.02$, Br = 0.1, $M = 0.01$. It is observed that the irreversibility distribution parameter Φ increases with increase in the values of N, λ_1, λ_2, λ_3 and s. Its value decreases with increase in Prandtl number Pr.

Table-II: Variation of irreversibility distribution parameter Φ

N	Pr	s	λ_3	λ_1, λ_2	Φ
40	7	0.5	0.01	0.01	1.59
40	11.4	0.5	0.01	0.01	1.51
40	7	0.5	0.015	0.01	4.20
40	7	0.2	0.01	0.01	0.97
60	7	0.5	0.01	0.01	8.09
40	7	0.5	0.01	0.02	4.22
40	11.4	0.2	0.01	0.02	3.93

5. Conclusions

1. The temperature profiles are influenced by variation in permeability of the lower plate. The results show an increase in the profiles with decrease in permeability.
2. The decrease in permeability of the upper plate leads to fall of temperature profiles.
3. The heat transfer shows a marked variation when the permeability of the lower plate is increased.
4. The magnetic parameter brings down the heat transfer profiles of both the plates.
5. The total entropy generated decreases as the plates move apart.

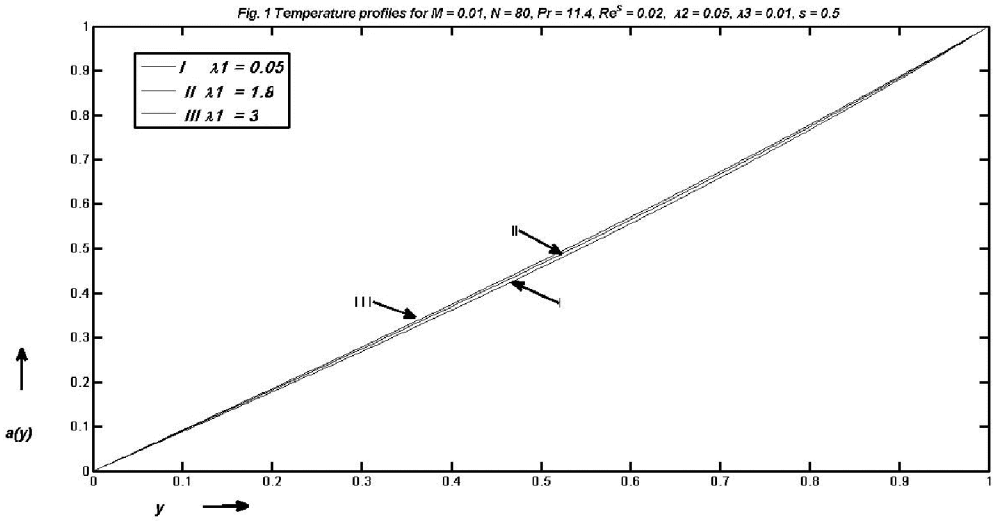

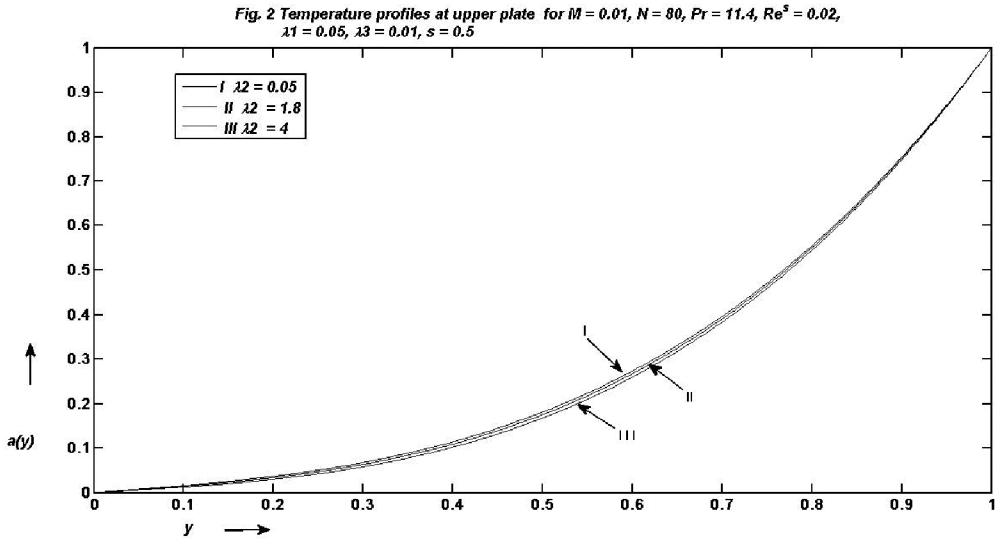

Fig. 3 Heat transfer profiles at the lower plate for M = 0.01, N = 80, Re^S = 0.02, λ2 = 0.05, s = 0.5

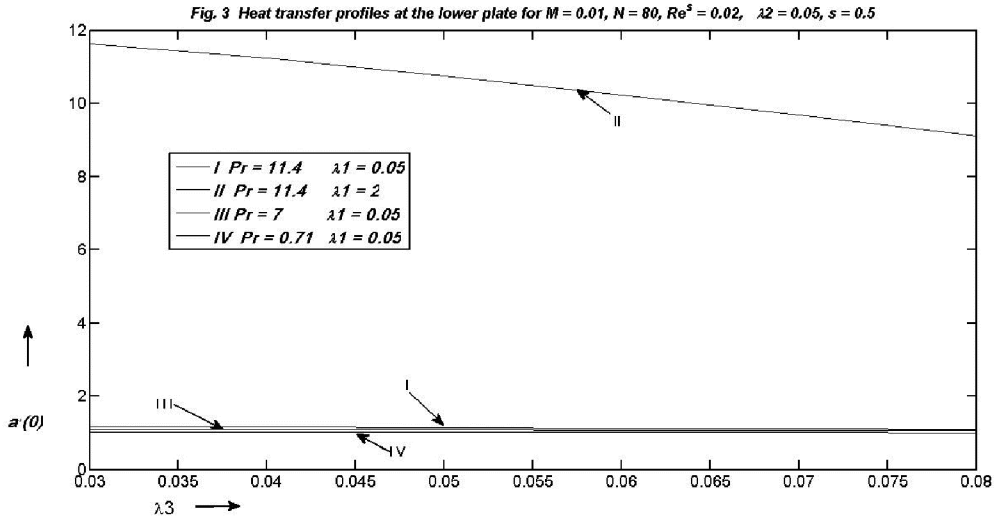

Fig. 4 Heat transfer profiles at the lower plate for N = 80,Pr = 11.4, Re^S = 0.02 λ1=λ2 = 0.05, s = 0.5

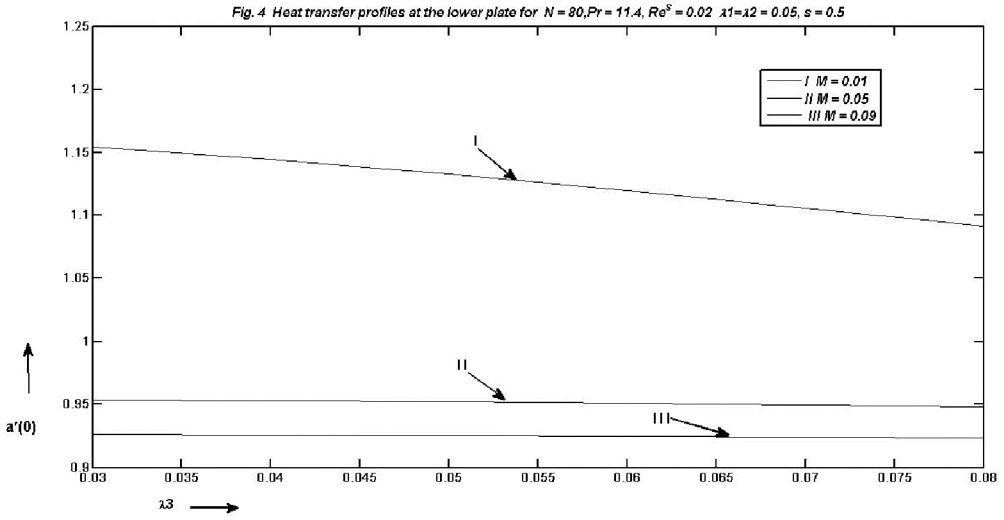

Fig. 5 Heat tranfer profiles at the upper plate for M = 0.01, N = 80, Re^S = 0.02, λ1 = 0.05, s = 0.5

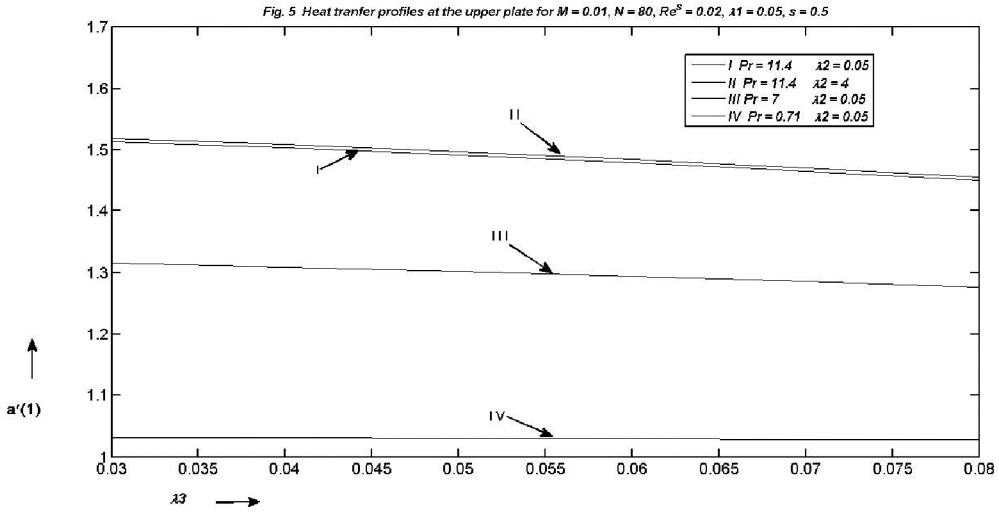

Fig. 6 Heat transfer profiles at the upper plate for N = 80, Pr = 11.4, Re^S = 0.02, λ1=λ2 = 0.05, s = 0.5

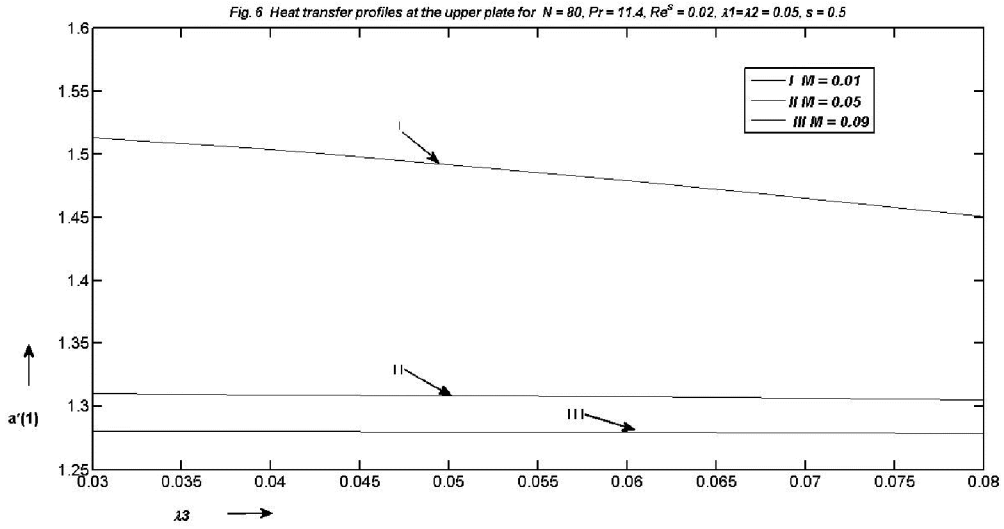

Fig. 7 Ns1 versus y with M = 0.01, N = 80, Pr = 7, Re^S = 0.02, λ1 = λ2 = 0.05,λ3 = 0.01, s = 0.5

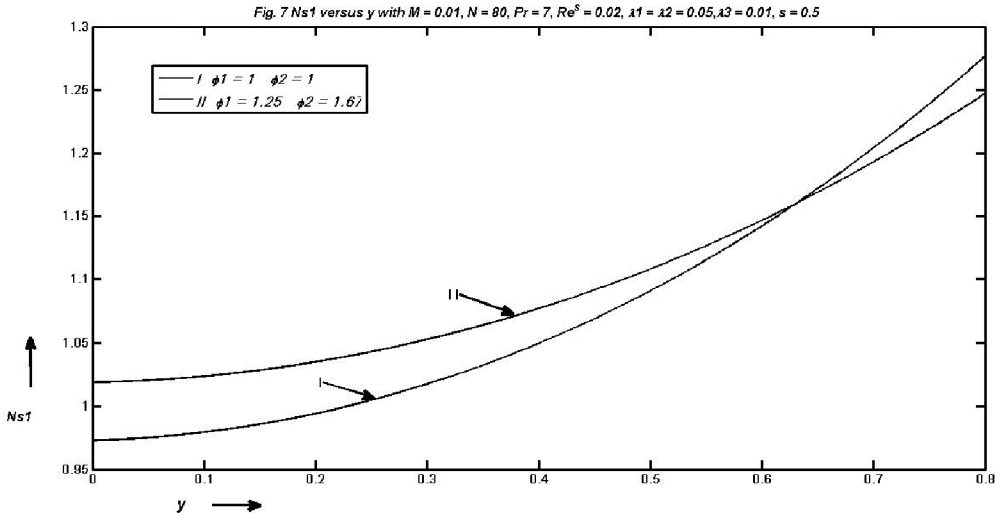

Fig. 8 Ns2 versus y with Br = 0.1, M = 0.01, N = 80, Pr = 7, Re^S = 0.02, λ1 = λ2 = 0.05,λ3 = 0.01, s = 0.5

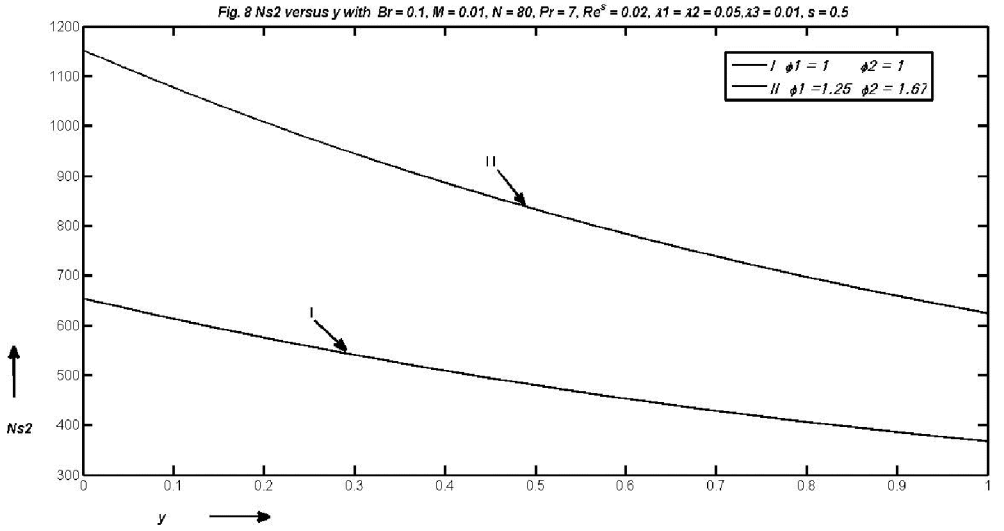

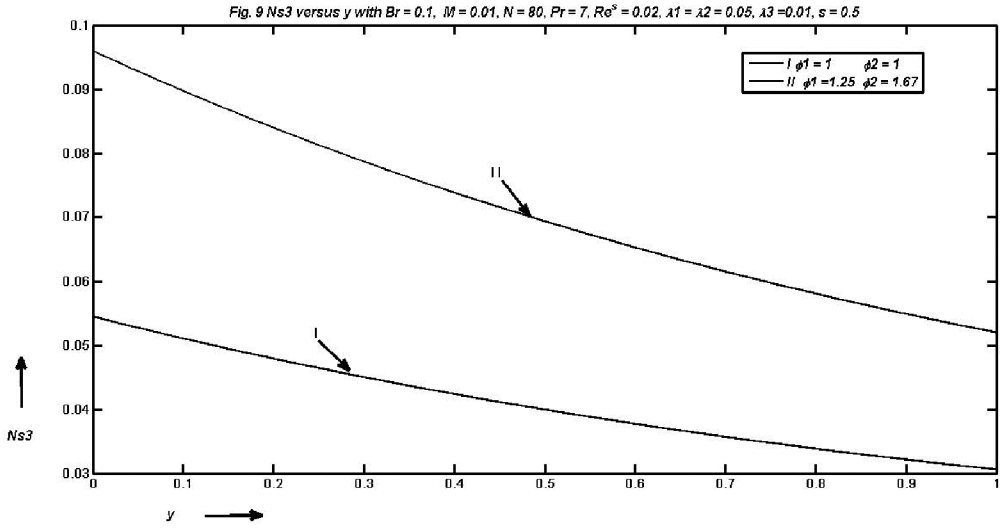

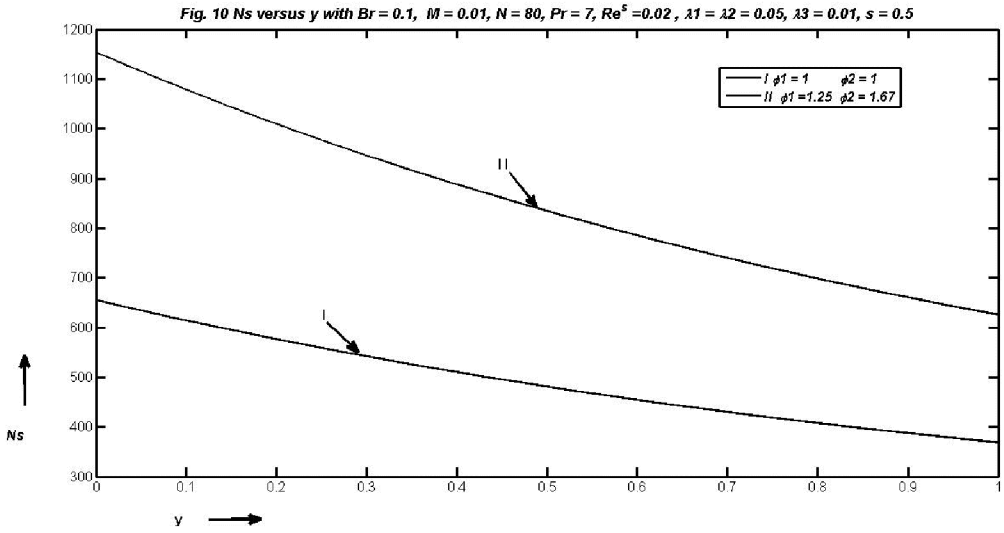

References

[1] Aristov, S. N. and Gitman, I. M. (2002). Viscous flow between two moving parallel disks: Exact solutions and stability analysis, *Journal of Fluid Mechanics* **46,** 209-215.

[2] Bhatt, B. S. and Hamza, E.A. (1996). Similarity solution for the squeezed film flow between two rotating naturally permeable discs, *Zeitschrift für Angewandte Mathematik und Mechanik* **76** (5), 291-299.

[3] Brinkman, H. C. (1947). A calculation of the viscous force exerted by a flowing fluid on a dense swarm of particles, *Applied Scientific Research* **1A**, 27-34.

[4] Chauhan, D. S. and Kumar, V. (2009). Effects of slip conditions on forced convection and entropy generation in a circular channel occupied by a highly porous medium: Darcy extended Brinkman-Forchheimer model, *Turkish Journal of Engineering and Environmental Science* **33,** 91-104.

[5] Erbay, L. B., Ercan, M. S., Sulus, B., Yalcin, M. M. (2003). Entropy generation during fluid flow between two parallel plates with moving bottom plate, *Entropy* **5** (5), 506-518.

[6] Gupta, P. S. and Gupta, A.S. (1977). Squeezing flow between parallel plates, *Lubrication and Wear* **45**(2), 177-185.

[7] Hamza, E. A. (1992). Unsteady flow between two disks with heat transfer in the presence of a magnetic field, *Journal of Physics D: Applied Physics* **25**, 1425-1431.

[8] Hayat, T., Yousaf, A., Mustafa, M., and Obaidat, S. (2011). MHD squeezing flow of second grade fluid between two parallel disks, *International Journal for Numerical Methods in Fluids*, doi: 10.1002/fld. 2565.

[9] Hunt, J. B. (1966). Pressure distribution in a plane fluid film subject to normal sinusoidal excitation, *Nature,* 1137-1139.

[10] Kuhn, E. C. and Yates, C.C. (1964). Fluid inertia effect on the film pressure between axially oscillating parallel circular plates, *ASLE Transactions* **7**, 299-303.

[11] Lygren, M. and Andersson, H. I. (2001). Turbulent flow between a rotating and stationary disk, *Journal of Fluid Mechanics* **426**, 297-326.

[12] Mohais, R. E. (2007), *Heat Transfer Studies of Coupled Fluid Flow within Porous Media*, Ph.D. Thesis, The University of the West Indies.

[13] Ozkol, I., Arikoglu, A. and Komurgoz, G. (2008). Effect of slip on entropy generation in a single rotating disk in MHD flow, *Applied Energy* **85**, 1225-1236.

[14] Rajvanshi, S. C. (1971). The flow between two parallel infinite disks, both subjected to normal sinusoidal oscillations, *Proc. Nat. Acad. Sci.*, India, **41**A, 209-219.

[15] Rajvanshi, S. C. (1981). Effect of axial current induced pinch and velocity slip on the squeeze-film behavior for porous annular disks, *Proc. Nat. Acad. Sci., India*, **51**A (3), 350-358.

[16] Rashidi, M. M., Shahmohamadi, H. and Dinarvand, S. (2008). Analytic approximate solutions for unsteady two-dimensional and axisymmetric squeezing flows between parallel plates, *Mathematical Problems in Engineering*, doi: 10.1155/2008/935095,1-13.

[17] Rukmani, R. and Usha, R. (1994). Arbitrary squeeze flow between two disks, *International Journal of Mathematics and Mathematical Sciences* **17** (4), 779-782.

[18] Saini, B. S. (2008). Flow between two parallel disks, one of which is subjected to normal sinusoidal oscillation and the other highly permeable, *Bulletin of Pure and Applied Mathematics* **2** (1), 30-46.

[19] Terrill, R. M. (1969). The flow between two parallel circular disks, one of which is subjected to normal sinusoidal oscillation, *Transactions of the ASME, Journal of Lubrication Technology* **91,** 126-131.

[20] Usha, R. and Vasudevan, S. (1993). A similar flow between two rotating discs in the presence of a magnetic field, *Journal of Applied Mechanics* **60,** 704-714.

[21] Wang, C. Y. (1976). The squeezing of fluid between two plates, *Journal of Applied Mechanics* **43**(4), 579-583.